Published in final edited form as:
*Cell Calcium*. 2009 July ; 46(1): 49–55. doi:10.1016/j.ceca.2009.04.002.

# Store-operated $Ca^{2+}$ influx and subplasmalemmal mitochondria

**Marek K. Korzeniowski**[a], **Gergö Szanda**[b], **Tamas Balla**[a], and **András Spät**[b,c,*]

a *Section on Molecular Signal Transduction, Program on Developmental Neuroscience, NICHD, NIH, Bethesda, MD, USA*

b *Dept. of Physiology, Semmelweis University, Budapest, Hungary*

c *Laboratory of Neurobiochemistry and Molecular Physiology, Hungarian Academy of Sciences, Budapest, Hungary*

## Abstract

Calcium depletion of the endoplasmic reticulum (ER) induces oligomerisation, *puncta* formation and translocation of the ER $Ca^{2+}$ sensor proteins, STIM1 and −2 into plasma membrane (PM)-adjacent regions of the ER, where they activate the Orai1, −2 or −3 proteins present in the opposing PM. These proteins form ion channels through which store-operated $Ca^{2+}$ influx (SOC) occurs. Calcium ions exert negative feed-back on SOC. Here we examined whether subplasmalemmal mitochondria, which reduce this feed-back by $Ca^{2+}$ uptake, are located within or out of the high-$Ca^{2+}$ microdomains (HCMDs) formed between the ER and plasmalemmal Orai1 channels. For this purpose, COS-7 cells were co-transfected with Orai1, STIM1 labelled with YFP or mRFP and the mitochondrially targeted $Ca^{2+}$ sensitive fluorescent protein inverse Pericam. Depletion of ER $Ca^{2+}$ with ATP + thapsigargin (in $Ca^{2+}$-free medium) induced the appearance of STIM1 puncta in the ≤100 nm wide subplasmalemmal space, as examined with TIRF. Mitochondria were located either in the gaps between STIM1-tagged puncta or in remote, STIM1-free regions. After addition of $Ca^{2+}$ mitochondrial $Ca^{2+}$ concentration increased irrespective of the mitochondrion-STIM1 distance. These observations indicate that mitochondria are exposed to $Ca^{2+}$ diffused laterally from the HCMDs formed between the PM and the subplasmalemmal ER.

### Keywords

mitochondria; calcium; store-operated calcium entry; STIM1

## Introduction

Inositol 1,4,5-trisphosphate-induced $Ca^{2+}$ depletion of the ER induces $Ca^{2+}$ influx from the extracellular space, a process originally termed as ‘capacitative $Ca^{2+}$ influx’ [1]. This form of $Ca^{2+}$ entry, presently more often referred to as store-operated $Ca^{2+}$ influx (SOC) can also be induced by thapsigargin (Tg) [2] and other inhibitors of SERCA, the Ca. ATPase of the ER. The molecular basis of SOC has recently been unveiled by the discovery of two sets of proteins: STIM1 and −2, the $Ca^{2+}$-sensor membrane proteins of the ER [3–5] and Orai1, −2 and −3, plasma membrane (PM) proteins forming $Ca^{2+}$-selective channels [6–8]. Although additional

*Corresponding author: Phone: +36 20 825 4026. Fax: +36 1 266 7480., E-mail address: E-mail: spat@puskin.sote.hu (A. Spät).

channels may also be regulated by STIM proteins and contribute to SOC [9–11], STIM1 and Orai1 are necessary and sufficient components of the SOC mechanism in most cell types, including COS-7 cells examined in the present study. Upon depletion of ER luminal $Ca^{2+}$, STIM1 undergoes sequential oligomerisation with ensuing formation of clusters and translocation into PM-adjacent regions within the ER [3,5,12–14]. The STIM1 clusters in the ER induce multimerization of the plasmalemmal Orai1 molecules where the two molecules colocalise [14–17] allowing a dramatic increase in SOC [18,19].

The role of mitochondria in the control of SOC has been suggested by several observations. Since elevation of cytosolic $[Ca^{2+}]$ ($[Ca^{2+}]_c$) exerts negative feed-back on SOC [20], $Ca^{2+}$ sequestration by mitochondria will reduce this inhibition [21–23]. This action of mitochondria requires an energized state but does not involve changes in intracellular ATP, indicating that it may be accounted for by $Ca^{2+}$ uptake [24]. Indeed, SOC is more active in the vicinity of than far from subplasmalemmal mitochondria [25]. Also, sustained activity of SOC channels may require the translocation of mitochondria into subplasmalemmal regions [26].

Mitochondrial $Ca^{2+}$ uptake occurs via the Ruthenium Red-sensitive $Ca^{2+}$ uniporter, a highly selective inwardly rectifying channel that displays low affinity for $Ca^{2+}$ [27]. However, mitochondrial $Ca^{2+}$ sequestration does occur despite the low $Ca^{2+}$ affinity of the uniporter during stimulation with a $Ca^{2+}$ mobilising agonist. This is because of the rapidly forming but short-lived high-$Ca^{2+}$ microdomains (HCMDs) between the mouth of $IP_3$ receptor-channels and closely apposed mitochondria [28,29]. Mitochondrial $Ca^{2+}$ uptake during voltage-operated $Ca^{2+}$ influx has also been accounted for by the formation of HCMDs between the cytosolic mouth of the plasmalemmal channel and the apposing mitochondria [30–33]. However, the formation of such HCMDs may not be an absolute requirement for mitochondrial $Ca^{2+}$ uptake during SOC. Observations in glomerulosa, luteal, HeLa and H295R cells suggest that SOC may be followed by mitochondrial $Ca^{2+}$ uptake without the need for HCMD [34–38]. Therefore we examined whether subplasmalemmal mitochondria are in a location where SOC-induced HCMDs may be formed.

## Methods

### Cells

COS-7 cells were cultured on glass coverslips and transfected for 24 h with 0.5–0.5 μg plasmid DNA of Orai1 and mRFP-STIM1 and 1 μg mitochondrially-targeted inverse Pericam (i-Pericam) [39] per dish (~ $10^5$ cells), using Lipofectamine 2000. Orai1 and STIM1 plasmids transcription was driven by the thymidine kinase (TK) promoter of the herpes simplex virus as described [14].

### Confocal laser scanning microscopy

Confocal analysis was performed at 35°C in a modified Krebs-Ringer buffer containing (in mM): 120 NaCl, 4.7 KCl, 1.2 $CaCl_2$, 0.7 $MgSO_4$, 10 glucose, 10 sodium Hepes, pH 7.4, using a Zeiss LSM 510-META scanning confocal microscope and a 63x/1.4 objective. The optical slice was set at 1.5 μm. Data were acquired in multitrack mode with scanning in the frame mode using the 488 and 543 nm lasers and BP 505–545 and LP560 emission filters for YFP or mt-i-Pericam and Rhod-2 or mRFP, respectively.

### Total internal reflection fluorescent microscopy (TIRF)

TIRF analysis was performed at room temperature in an Olympus through the lens dual launch TIRF microscope system equipped with a Hammamatsu EM-CCD camera and a PlanApo 60x/1.45 objective. 488 or 568 nm lasers and 535/40 and 645/75 emission filters were used for the mt-i-Pericam and mRFP, respectively. The Openlab Software (Improvision) was used for data

acquisition, and the pictures were exported as TIFF files for processing with the Metamorph software (Molecular Devices). In some cases, the microscopic images were deconvoluted using a plugin (Iterative Deconvolve 3D) of ImageJ 1.37a.

### Statistics

Statistical data are expressed as means ± S.E.M. For the evaluation of co-localisation of STIM1 puncta and subplasmalemmal mitochondria Pearson's coefficient [40] was calculated after thresholding, applying a plugin of ImageJ 1.37a which excludes zero-zero pixels (Intensity Correlation Analysis). For curve fitting in Fig. 3 the spline/Lowess function of the Prism software was applied. Initial rate of $Ca^{2+}$ -induced decrease in i-Pericam fluorescence in mitochondria close to or far from STIM1-labelled ER was compared with ANOVA.

## Results and Discussion

In order to enhance the active sites of SOC in COS-7 cells, Orai-1 and fluorescent protein-tagged STIM1 proteins were co-expressed. To achieve only moderate levels of expression, these constructs were driven by the thymidine kinase (TK) promoter [14]. The ER $Ca^{2+}$ store was rapidly depleted by the addition of 50 μM ATP and 200 nM Tg to stimulate the endogenous metabotropic $P_{2Y}$ receptors and inhibit the SERCA $Ca^{2+}$ pump, respectively. $Ca^{2+}$ responses of the transfected cells in the cytosol and mitochondria were followed by confocal microscopy in regions of interest (ROIs) over the nucleus and over mitochondria, respectively, using the $Ca^{2+}$ sensitive fluorescent dye Rhod-2. The rate and extent of the translocation of STIM1 towards the cell periphery was estimated off-line by measuring YFP fluorescence in ROIs over the perinuclear ER and puncta-rich periphery, respectively. As shown in Fig. 1, addition of ATP + Tg in the presence of external $Ca^{2+}$, induced a rapid increase in $[Ca^{2+}]_c$ that was associated with a moderate rise in mitochondrial $[Ca^{2+}]$ ($[Ca^{2+}]_m$). This reflected the rapid $Ca^{2+}$ release from the ER. However, a second phase of the $Ca^{2+}$ response was observed with a slight delay, which was much more pronounced in the mitochondria than in the cytosol (note the different scales of cytosolic and mitochondrial Rhod-2 signals on the *y* axes in Fig. 1B !). The onset of this secondary $Ca^{2+}$ rise coincided with the translocation of STIM1 from the ER to the cell periphery and was, therefore, attributed to massive $Ca^{2+}$ influx via the expressed Orai1 channels. Based on these data it may be assumed that mitochondria are capable of a significant sequestration of the inflowing $Ca^{2+}$ and to some extent may protect the cytosol from very large $[Ca^{2+}]_i$ increases.

In subsequent experiments the effects of $Ca^{2+}$ depletion of the ER and increased $Ca^{2+}$ influx on $[Ca^{2+}]_m$ were studied with confocal- and TIRF microscopy, in order to determine whether the mitochondrial responses were dependent on the localization of the mitochondrion relative to that of STIM1. For this, cells were cotransfected with mRFP-STIM1 and a mitochondrially targeted inverse Pericam (i-Pericam) (Fig. 2). i-Pericam is a $Ca^{2+}$ sensitive protein displaying high fluorescence intensity at low $[Ca^{2+}]_m$ [39]. The application of i-Pericam was preferred over that of Rhod-2 because of its better suitability to detect mitochondria at low $[Ca^{2+}]_m$ which was critical in subsequent TIRF experiments. In the resting state, mRFP-STIM1 showed its usual ER localization with some association with microtubules as described in several previous studies [41,42]. The mitochondria could easily be detected due to their high fluorescence at to low $[Ca^{2+}]_m$. $Ca^{2+}$ depletion of the ER was induced with ATP + Tg in a $Ca^{2+}$-free medium (containing 100 μM EGTA). Within 2 minutes of drug application, mRFP fluorescence became highly punctated indicating the formation of STIM1 clusters and enrichment in close proximity to the PM (Fig. 2A). $Ca^{2+}$ influx was then initiated by the addition of 2 mM $Ca^{2+}$ to the medium so that the effect of $Ca^{2+}$ influx could be studied without $Ca^{2+}$ release from the ER $Ca^{2+}$ stores. Within 10 s after the addition of $Ca^{2+}$, i-Pericam fluorescence rapidly decreased reflecting the

SOC-evoked increase in $[Ca^{2+}]_m$ (Fig. 2B). These experiments showed that i-Pericam is capable of reporting the rapid $Ca^{2+}$ rise in the mitochondria associated with $Ca^{2+}$ influx.

Next, the position of the mitochondria relative to the STIM1 puncta within the ≤100 nm wide subplasmalemmal space was examined with TIRF microscopy. After ER $Ca^{2+}$ depletion by the addition of ATP + Tg (in a $Ca^{2+}$-free medium containing 100 μM EGTA), mRFP-STIM1 puncta were detectable at the vicinity of the PM, and a few mitochondria showing i-Pericam fluorescence could also be located in this space. Importantly, the PM-close mitochondria showed no preferential localization close to the STIM1 puncta, but were found either in between the STIM1 patches or further away, in STIM1-free regions (Fig. 3A). Very few mitochondria could be detected contacting or at least partially overlapping with red fluorescing (mRFP) pixels. This was clearly demonstrable in pixel intensity profiles where pixels with high intensities in both green and red channels were very rarely detected. Colocalisation was also statistically estimated. Pearson's coefficient which may change between +1 (colocalisation) and −1 (exclusion), was −0.750 ± 0.105 (means ± S.E.M.) in the original images and −0.912 ± 0.026 after deconvolution (n=5), confirming the lack of colocalisation of mRFP and i-Pericam.

Since $Ca^{2+}$ influx probably saturates i-Pericam [39] the amplitude of mitochondrial $Ca^{2+}$ response could not be accurately measured. Therefore we compared the initial rate of the fall of dye fluorescence (expressed as $\Delta F/F_o$ per second where $F_o$ is F before adding $Ca^{2+}$) in mitochondria far from ER (i.e. more than 10 pixels distance between the two organelles) and those close to ER. There was no statistical difference in the rates estimated for 12 far and 12 close mitochondria (selected in 3 cells) ($p = 0.125$). Similarly, no difference was observed when fluorescence intensities were expressed as per cent of max-min values (Fig. 3B). (These experiments were performed at room temperature to allow detection of small differences, therefore the $Ca^{2+}$ response of mitochondria was somewhat slower than observed at 35 C.)

The relationship between mRFP-STIM1 and i-Pericam in ER-$Ca^{2+}$-depleted cells was further evaluated with scatter plots. In $Ca^{2+}$ depleted cells high i-Pericam fluorescence values (requiring good i-Pericam expression and low $[Ca^{2+}]_m$) were found in the low range of STIM1 fluorescence. Following readdition of $Ca^{2+}$ the green fluorescence intensities of these pixels was drastically reduced, indicating that these pixels corresponded to functioning mitochondria capable of $Ca^{2+}$ uptake (Fig. 4). The prominent fall of i-Pericam fluorescence across the spectrum of pixels with red fluorescence upon the induction of $Ca^{2+}$ also confirmed the conclusion that mitochondria show equally good $Ca^{2+}$ responses whether located in between STIM1 puncta or in remote, STIM1-free regions.

Collectively, these results did not indicate the existence of preferential spatial positioning of mitochondria close to the STIM1/Orai1 formed $Ca^{2+}$ entry sites. HCMDs is spatially and temporally defined local elevations of $[Ca^{2+}]_c$ around the mouth of a $Ca^{2+}$ release channel or a plasmalemmal $Ca^{2+}$ channel. Its formation is allowed by a low diffusion rate of $Ca^{2+}$ (due to immobile cytosolic $Ca^{2+}$ buffers) and facilitated by a physical barrier for diffusion, the subplasmalemmal ER sites containing STIM1 puncta in our case. This way SOC-related HCMDs theoretically could be formed between Orai1 clusters and the apposing ER membrane rich in STIM1 puncta. Given the limited distance between the STIM1-labelled ER membrane and the Orai1 in the apposing PM, which was estimated to be in the range of 10–25 nm [14, 43], this space is too narrow to accommodate a mitochondrion. Therefore, mitochondria may be exposed to $Ca^{2+}$ diffusing only laterally from the HCMDs during SOC. This means that subplasmalemmal mitochondria are exposed to $Ca^{2+}$ at concentrations probably exceeding that of the global cytosolic $[Ca^{2+}]$ increase. The nearer they are to the HCMDs formed around the orifice of Orai channels the higher $[Ca^{2+}]$ they are exposed to, but at least in non-excitable cells, even this local $[Ca^{2+}]$ may not attain the high values found in HCMDs close to the ER

$Ca^{2+}$ release sites. Whereas the estimated subplasmalemmal [$Ca^{2+}$] values ranged between 20 and 300 μM in various excitable cells [44–47] subplasmalemmal [$Ca^{2+}$] amounted to only ~1.6 μM in the non-excitable endothelial cells [25]. Therefore in non-excitable cells the cell-type specific threshold of mitochondrial $Ca^{2+}$ uptake (cf. [48]) rather than the position relative to the SOC site may determine to what an extent mitochondria can modify subplasmalemmal $[Ca^{2+}]_c$ during SOC.

## Acknowledgments

Mt-inverse Pericam was kindly gifted by Prof. A. Miyawaki (Saitama, Japan). The confocal imaging was performed at the Microscopy & Imaging Core of the National Institute of Child Health and Human Development, NIH with the kind assistance of Drs. Vincent Schram and James T. Russell. This research was supported in part by the Intramural Research Program of the National Institute of Child Health and Human Development of the National Institutes of Health.

## References

1. Putney JW Jr. A model for receptor-regulated calcium entry. Cell Calcium 1986;7:1–12. [PubMed: 2420465]
2. Takemura H, Hughes AR, Thastrup O, Putney JW Jr. Activation of calcium entry by the tumor promoter thapsigargin in parotid acinar cells. J Biol Chem 1989;264:12266–12271. [PubMed: 2663854]
3. Liou J, Kim ML, Heo WD, et al. STIM is a $Ca^{2+}$ sensor essential for $Ca^{2+}$-store-depletion-triggered $Ca^{2+}$ influx. Curr Biol 2005;15:1235–1241. [PubMed: 16005298]
4. Roos J, DiGregorio PJ, Yeromin AV, et al. STIM1, an essential and conserved component of store-operated $Ca^{2+}$ channel function. J Cell Biol 2005;169:435–445. [PubMed: 15866891]
5. Zhang SL, Yu Y, Roos J, et al. STIM1 is a $Ca^{2+}$ sensor that activates CRAC channels and migrates from the $Ca^{2+}$ store to the plasma membrane. Nature 2005;437:902–905. [PubMed: 16208375]
6. Feske S, Gwack Y, Prakriya M, et al. A mutation in Orai1 causes immune deficiency by abrogating CRAC channel function. Nature 2006;441:179–185. [PubMed: 16582901]
7. Yeromin AV, Zhang SL, Jiang W, Yu Y, Safrina O, Cahalan MD. Molecular identification of the CRAC channel by altered ion selectivity in a mutant of Orai. Nature 2006;443:226–229. [PubMed: 16921385]
8. Zhang SL, Yeromin AV, Zhang XH, et al. Genome-wide RNAi screen of $Ca^{2+}$ influx identifies genes that regulate $Ca^{2+}$ release-activated $Ca^{2+}$ channel activity. Proc Natl Acad Sci U S A 2006;103:9357–9362. [PubMed: 16751269]
9. Philipp S, Trost C, Warnat J, et al. TRP4 (CCE1) protein is part of native calcium release-activated $Ca^{2+}$- like channels in adrenal cells. J Biol Chem 2000;275:23965–23972. [PubMed: 10816590]
10. Yuan JP, Zeng W, Huang GN, Worley PF, Muallem S. STIM1 heteromultimerizes TRPC channels to determine their function as store-operated channels. Nat Cell Biol 2007;9:636–645. [PubMed: 17486119]
11. Alicia S, Angelica Z, Carlos S, Alfonso S, Vaca L. STIM1 converts TRPC1 from a receptor-operated to a store-operated channel: moving TRPC1 in and out of lipid rafts. Cell Calcium 2008;44:479–491. [PubMed: 18420269]
12. Liou J, Fivaz M, Inoue T, Meyer T. Live-cell imaging reveals sequential oligomerization and local plasma membrane targeting of stromal interaction molecule 1 after $Ca^{2+}$ store depletion. Proc Natl Acad Sci U S A 2007;104:9301–9306. [PubMed: 17517596]
13. Luik RM, Wang B, Prakriya M, Wu MM, Lewis RS. Oligomerization of STIM1 couples ER calcium depletion to CRAC channel activation. Nature 2008;454:538–542. [PubMed: 18596693]
14. Várnai P, Tóth B, Tóth DJ, Hunyady L, Balla T. Visualization and manipulation of plasma membrane-endoplasmic reticulum contact sites indicates the presence of additional molecular components within the STIM1-Orai1 Complex. J Biol Chem 2007;282:29678–29690. [PubMed: 17684017]
15. Luik RM, Wu MM, Buchanan J, Lewis RS. The elementary unit of store-operated $Ca^{2+}$ entry: local activation of CRAC channels by STIM1 at ER-plasma membrane junctions. J Cell Biol 2006;174:815–825. [PubMed: 16966423]

16. Xu P, Lu J, Li Z, Yu X, Chen L, Xu T. Aggregation of STIM1 underneath the plasma membrane induces clustering of Orai1. Biochem Biophys Res Commun 2006;350:969–976. [PubMed: 17045966]
17. Penna A, Demuro A, Yeromin AV, et al. The CRAC channel consists of a tetramer formed by Stim-induced dimerization of Orai dimers. Nature 2008;456:116–120. [PubMed: 18820677]
18. Mercer JC, Dehaven WI, Smyth JT, et al. Large store-operated calcium-selective currents due to co-expression of Orai1 or Orai2 with the intracellular calcium sensor, Stim1. J Biol Chem 2006;281:24979. [PubMed: 16807233]
19. Peinelt C, Vig M, Koomoa DL, et al. Amplification of CRAC current by STIM1 and CRACM1 (Orai1). Nat Cell Biol 2006;8:771–773. [PubMed: 16733527]
20. Parekh AB. Slow feedback inhibition of calcium release-activated calcium current by calcium entry. J Biol Chem 1998;273:14925–14932. [PubMed: 9614097]
21. Hoth M, Fanger CM, Lewis RS. Mitochondrial regulation of store-operated calcium signaling in T lymphocytes. J Cell Biol 1997;137:633–648. [PubMed: 9151670]
22. Gilabert JA, Bakowski D, Parekh AB. Energized mitochondria increase the dynamic range over which inositol 1,4,5-trisphosphate activates store-operated calcium influx. EMBO J 2001;20:2672–2679. [PubMed: 11387202]
23. Malli R, Frieden M, Osibow K, et al. Sustained $Ca^{2+}$ transfer across mitochondria is essential for mitochondrial $Ca^{2+}$ buffering, sore-operated $Ca^{2+}$ entry, and $Ca^{2+}$ store refilling. J Biol Chem 2003;278:44769–44779. [PubMed: 12941956]
24. Glitsch MD, Bakowski D, Parekh AB. Store-operated $Ca^{2+}$ entry depends on mitochondrial $Ca^{2+}$ uptake. Embo J 2002;21:6744–6754. [PubMed: 12485995]
25. Malli R, Frieden M, Osibow K, Graier WF. Mitochondria efficiently buffer subplasmalemmal Ca2+ elevation during agonist stimulation. J Biol Chem 2003;278:10807–10815. [PubMed: 12529366]
26. Quintana A, Schwarz EC, Schwindling C, Lipp P, Kaestner L, Hoth M. Sustained activity of calcium release-activated calcium channels requires translocation of mitochondria to the plasma membrane. J Biol Chem 2006;281:40302–40309. [PubMed: 17056596]
27. Kirichok Y, Krapivinsky G, Clapham DE. The mitochondrial calcium uniporter is a highly selective ion channel. Nature 2004;427:360–364. [PubMed: 14737170]
28. Rizzuto R, Brini M, Murgia M, Pozzan T. Microdomains with high $Ca^{2+}$ close to $IP_3$-sensitive channels that are sensed by neighboring mitochondria. Science 1993;262:744–747. [PubMed: 8235595]
29. Moreau B, Nelson C, Parekh AB. Biphasic regulation of mitochondrial $Ca^{2+}$ uptake by cytosolic $Ca^{2+}$ concentration. Curr Biol 2006;16:1672–1677. [PubMed: 16920631]
30. Rutter GA, Theler JM, Murgia M, Wollheim CB, Pozzan T, Rizzuto R. Stimulated $Ca^{2+}$ influx raises mitochondrial free $Ca^{2+}$ to supramicromolar levels in a pancreatic b-cell line. Possible role in glucose and agonist-induced insulin secretion. J Biol Chem 1993;268:22385–22390. [PubMed: 8226749]
31. Kennedy ED, Rizzuto R, Theler JM, et al. Glucose-stimulated insulin secretion correlates with changes in mitochondrial and cytosolic $Ca^{2+}$ in aequorin-expressing INS-1 cells. J Clin Invest 1996;98:2524–2538. [PubMed: 8958215]
32. Pivovarova NB, Hongpaisan J, Andrews SB, Friel DD. Depolarization-induced mitochondrial Ca accumulation in sympathetic neurons: Spatial and temporal characteristics. J Neurosci 1999;19:6372–6384. [PubMed: 10414966]
33. Alonso MT, Villalobos C, Chamero P, Alvarez J, Garcia-Sancho J. Calcium microdomains in mitochondria and nucleus. Cell Calcium 2006;40:513–525. [PubMed: 17067669]
34. Rohács T, Tory K, Dobos A, Spät A. Intracellular calcium release is more efficient than calcium influx in stimulating mitochondrial NAD(P)H formation in adrenal glomerulosa cells. Biochemical Journal 1997;328:525–528. [PubMed: 9371711]
35. Collins TJ, Lipp P, Berridge MJ, Bootman MD. Mitochondrial $Ca^{2+}$ uptake depends on the spatial and temporal profile of cytosolic $Ca^{2+}$ signals. J Biol Chem 2001;276:26411–26420. [PubMed: 11333261]
36. Szabadkai G, Pitter JG, Spät A. Cytoplasmic $Ca^{2+}$ at low submicromolar concentration stimulates mitochondrial metabolism in rat luteal cells. Pflügers Arch 2001;441:678–685.

37. Pitter JG, Maechler P, Wollheim CB, Spät A. Mitochondria respond to $Ca^{2+}$ already in the submicromolar range: correlation with redox state. Cell Calcium 2002;31:97–104. [PubMed: 11969250]
38. Szanda G, Koncz P, Várnai P, Spät A. Mitochondrial $Ca^{2+}$ uptake with and without the formation of high-$Ca^{2+}$ microdomains. Cell Calcium 2006;40:527–538. [PubMed: 17069884]
39. Nagai T, Sawano A, Park ES, Miyawaki A. Circularly permuted green fluorescent proteins engineered to sense $Ca^{2+}$ Proc Natl Acad Sci 2001;98:3197–3202. [PubMed: 11248055]
40. Bolte S, Cordelieres FP. A guided tour into subcellular colocalization analysis in light microscopy. J Microsc 2006;224:213–232. [PubMed: 17210054]
41. Smyth JT, Dehaven WI, Bird GS, Putney JW Jr. Role of the microtubule cytoskeleton in the function of the store-operated $Ca^{2+}$ channel activator STIM1. J Cell Sci 2007;120:3762–3771. [PubMed: 17925382]
42. Grigoriev I, Gouveia SM, van der Vaart B, et al. STIM1 Is a MT-Plus-End-Tracking Protein Involved in Remodeling of the ER. Curr Biol 2008;18:177–182. [PubMed: 18249114]
43. Wu MM, Buchanan J, Luik RM, Lewis RS. $Ca^{2+}$ store depletion causes STIM1 to accumulate in ER regions closely associated with the plasma membrane. J Cell Biol 2006;174:803–813. [PubMed: 16966422]
44. Llinas R, Sugimori M, Silver RB. Microdomains of high calcium concentration in a presynaptic terminal. Science 1992;256:677–679. [PubMed: 1350109]
45. Heidelberger R, Heinemann C, Neher E, Matthews G. Calcium dependence of the rate of exocytosis in a synaptic terminal. Nature 1994;371:513–515. [PubMed: 7935764]
46. Marsault R, Murgia M, Pozzan T, Rizzuto R. Domains of high Ca2+ beneath the plasma membrane of living A7r5 cells. EMBO J 1997;16:1575–1581. [PubMed: 9130702]
47. Montero M, Alonso MT, Carnicero E, et al. Chromaffin-cell stimulation triggers fast millimolar mitochondrial $Ca^{2+}$ transients that modulate secretion. Nat Cell Biol 2000;2:57–61. [PubMed: 10655583]
48. Spät A, Szanda G, Csordás G, Hajnóczky G. High- and low-calcium-dependent mechanisms of mitochondrial calcium signalling. Cell Calcium 2008;44:51–63. [PubMed: 18242694]

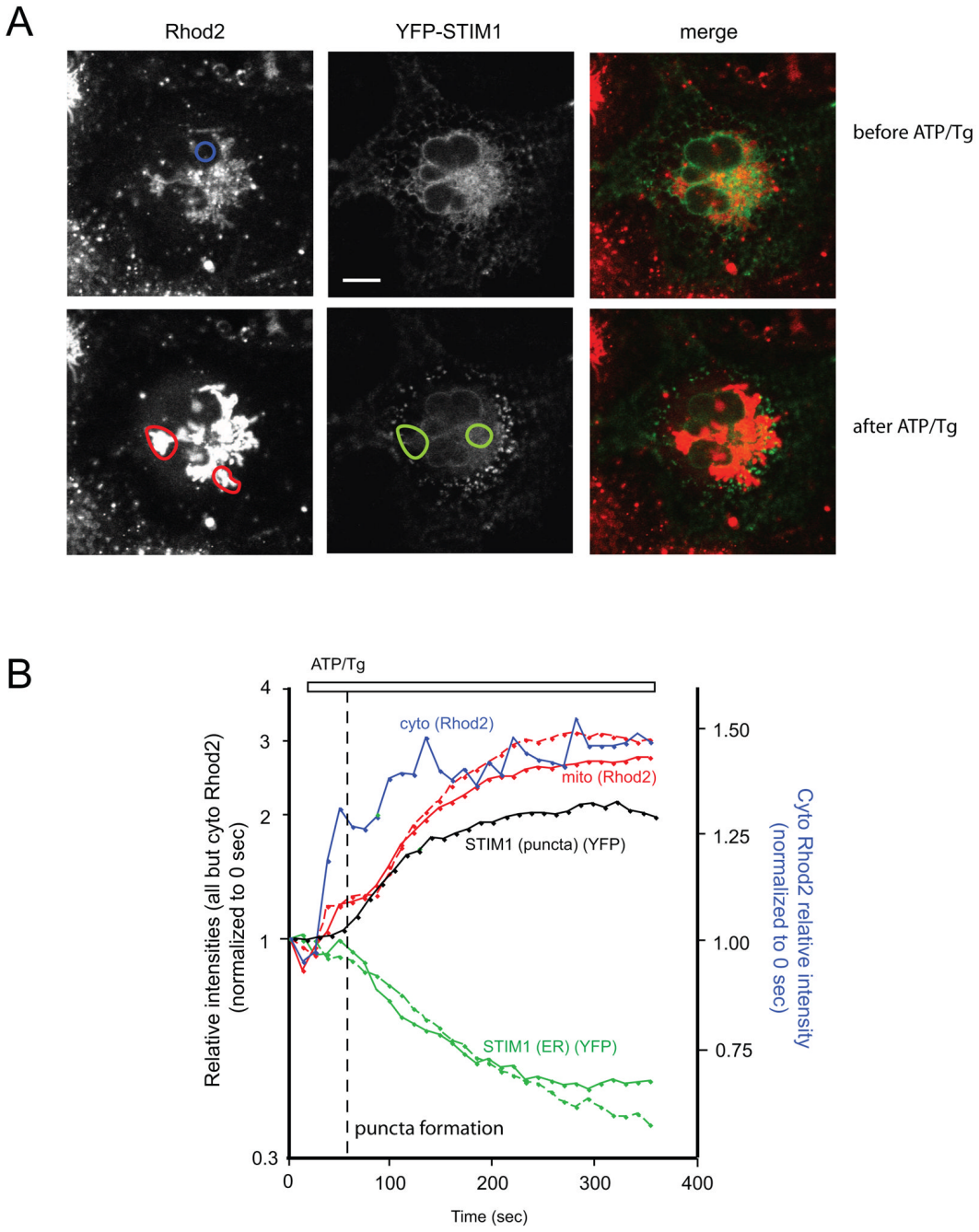


**Fig. 1.**

Confocal image of a Rhod-2 loaded COS-7 cell transfected with TK-YFP-STIM1 and untagged Orai1. (A) Upper row: control, lower row: 5 min after the addition 50 μM ATP and 200 nM Tg in normal $Ca^{2+}$ containing medium. Note the large increase in Rhod-2 fluorescence (left panels) and the formation of STIM1 puncta in the cell periphery (middle panels). The bar shows 10 μm (B): Quantitation of fluorescence changes during the whole time-course of this experiment. Cytoplasmic [$Ca^{2+}$] (cyto, blue trace) was measured with Rhod-2 fluorescence monitored over the nuclear area (blue circle). Mitochondrial [$Ca^{2+}$] (red traces) was measured with Rhod-2 at two selected areas over mitochondria (red circles). STIM1 translocation was indicated either by the decreased YFP-STIM1 fluorescence in two central ER areas (green

circles) of the cell (green traces) or by the increased average fluorescence of several puncta at the peripheral region of the cell (selected areas too small to show in the picture) (black trace). All fluorescence intensities were normalized to 0 sec. The dotted line shows the assumed onset of SOC (cf. [14]). Note the two-phased increase in mitochondrial [$Ca^{2+}$], a small increase associated with the rapid $Ca^{2+}$ release from the ER and a slightly delayed massive $Ca^{2+}$ uptake corresponding to the large SOC due to STIM1/Orai1 expression. The latter coincides with STIM1 translocation to the cell periphery.

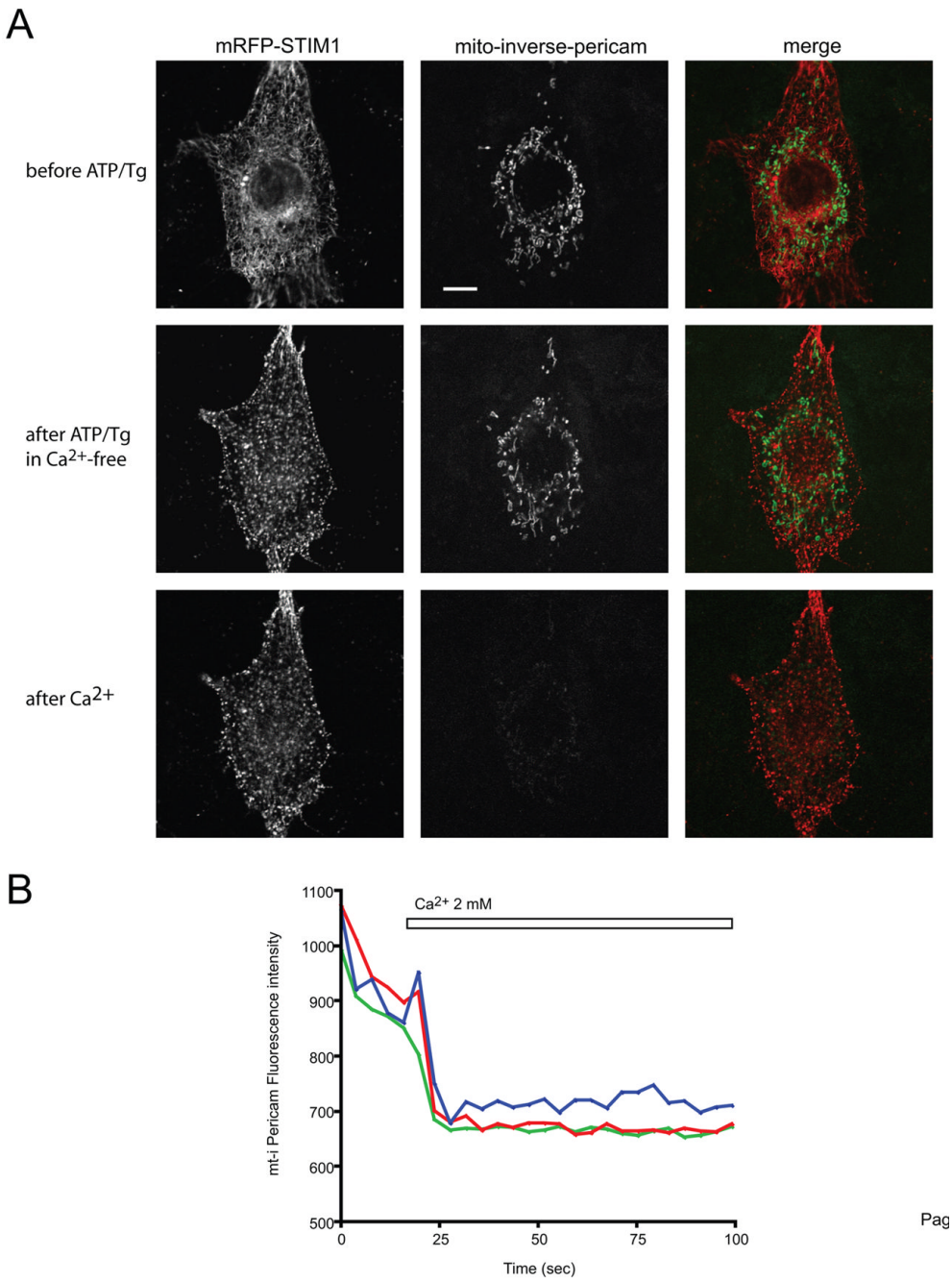


**Fig. 2.**

Confocal image of a COS-7 cell expressing mRFP-STIM1, untagged Orai1 and inverse-Pericam-targeted to the mitochondrial matrix. (A) Upper row: control, middle row: 2 min after stimulation with 50 μM ATP and 200 nM Tg in $Ca^{2+}$-free medium (note the formation of STIM1 puncta on the left panels), lower row: 2 min after the addition of 2 mM $Ca^{2+}$ (note the disappearance of i-Pericam fluorescence). The bar shows 10 μm (B) The lower panel shows the rapid fall of mitochondrially targeted i-Pericam (i.e. the increase in $[Ca^{2+}]_m$) in 3 separate mitochondrial ROIs in response to readdition of $Ca^{2+}$. (Performed at 35 C.)

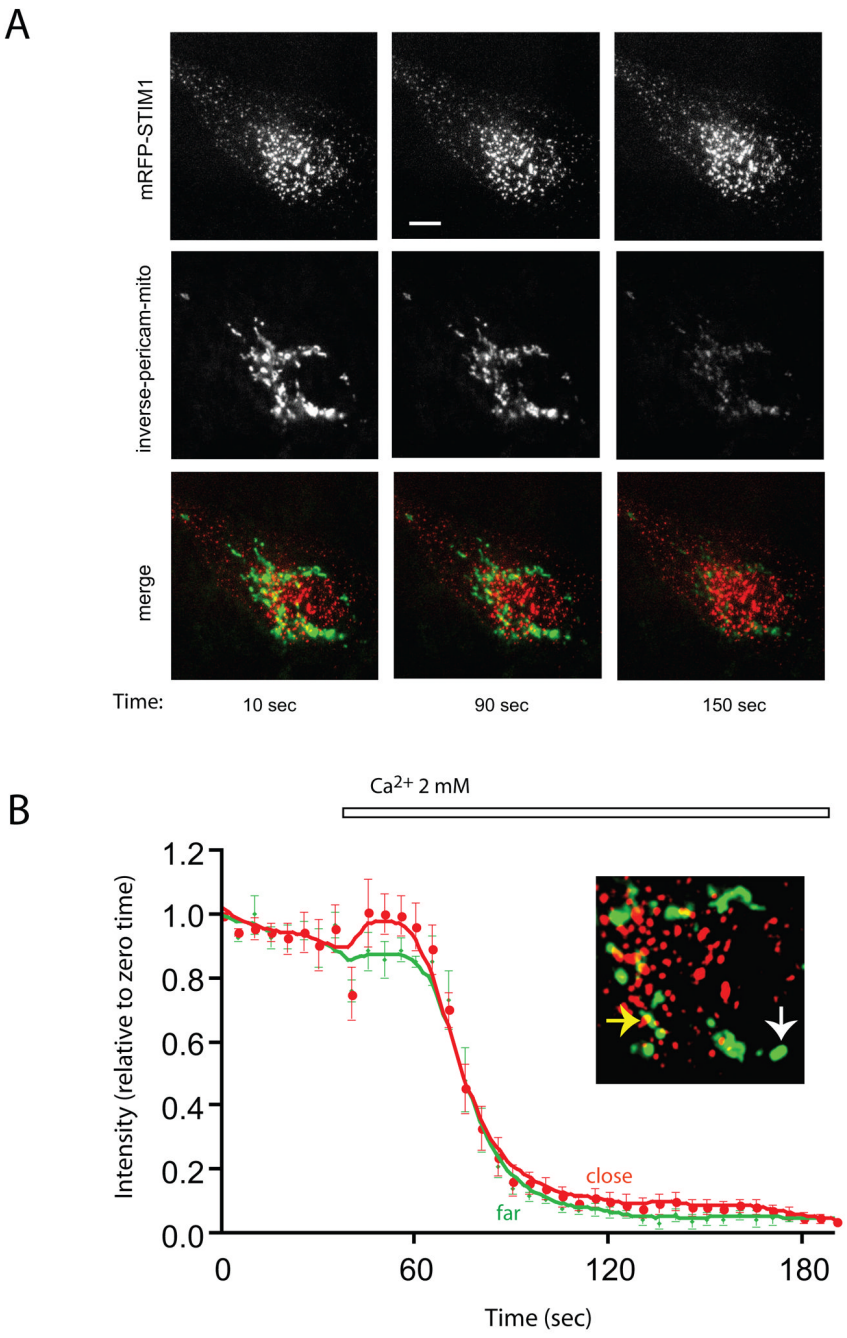


**Fig. 3.**

TIRF analysis (performed at room temperature) of COS-7 cells expressing mRFP-STIM1, untagged Orai1 and inverse-Pericam-targeted to the mitochondrial matrix. (A) This recording (representative for 5 cells) was started after treatment of cells with ATP + Tg in $Ca^{2+}$ -free medium (~ 9 min). The punctate appearance of STIM1 (upper row) shows that STIM1 is already translocated to the peripheral parts of the ER. Mitochondrial fluorescence (middle row) is high at this point as $Ca^{2+}$ influx cannot take place in the absence of external $Ca^{2+}$ (left pictures). $Ca^{2+}$ uptake was induced with the addition of 2 mM $Ca^{2+}$, and mitochondrial $Ca^{2+}$ uptake is indicated by the decreased fluorescence intensity of the mitochondrially targeted inverse Pericam (middle and right pictures of the middle row). The bar shows 10 μm (B) Quantitative

analysis of fluorescence changes during the time-course of this recording. Red and green traces show changes in the i-Pericam fluorescence intensity in selected mitochondria close to (contacting) or far (more than 10 pixels distance) from mRFP-STIM1 fluorescence. The data points for each ROI were expressed as per cent of max-min values and these values were averaged (means ± S.E.M., n= 4). The enlarged image shows an example for a close (yellow arrow) or far (white arrow) mitochondrion relative to active STIM1 areas.

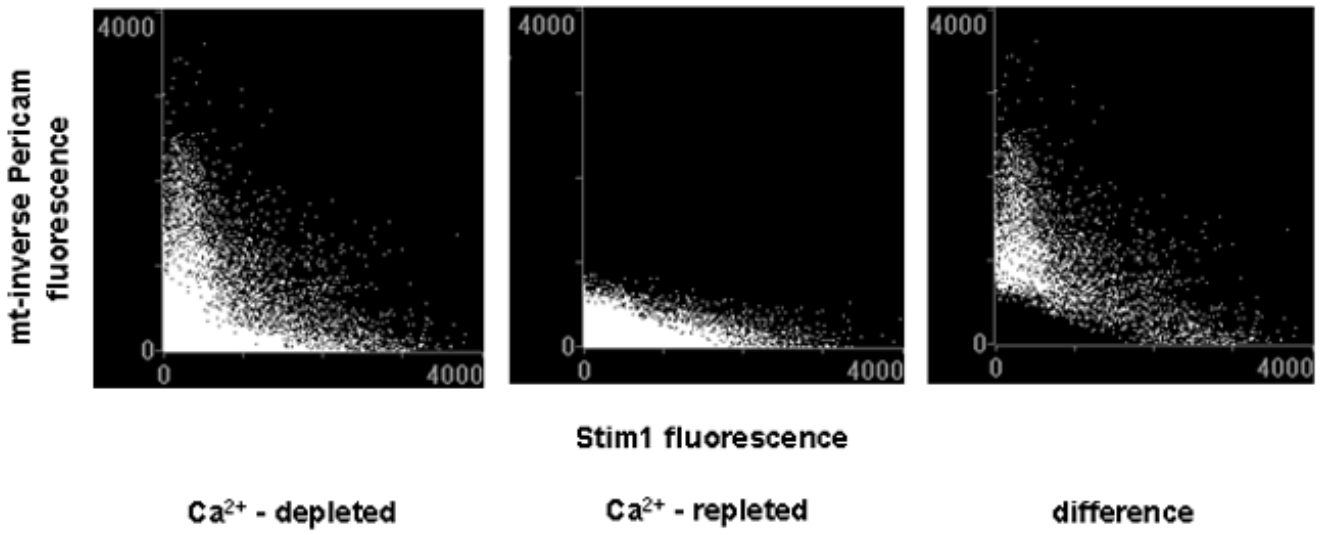


**Fig. 4.**

Scatter plot showing the fluorescence intensity of mitochondrially targeted i-Pericam (Y axis) as a function of the fluorescence intensity of STIM1-mRFP (X axis) in the cell shown in Fig. 3. Left panel: 9 min after $Ca^{2+}$ depletion induced with ATP + Tg, middle panel: 1 min after the addition 2 mM $Ca^{2+}$, right panel: pixels disappeared after the addition of $Ca^{2+}$ (the middle scatter plot subtracted from the left one).